Uncertainty Aware Structural Topology Optimization Via a Stochastic Reduced Order Model Approach

Miguel A. Aguiló[1] and James E. Warner[2]

[1]Simulation Modeling Sciences; Sandia National Laboratories; P.O. Box 5800, Albuquerque, NM 87185-0380; Ph: (505) 845-8964; email: maguilo@sandia.gov
[2]NASA Langley Research Center; Durability, Damage Tolerance, & Reliability Branch; Hampton, VA 23666; Ph: (757) 864-9041; email: james.e.warner@nasa.gov

ABSTRACT

This work presents a stochastic reduced order modeling strategy for the quantification and propagation of uncertainties in topology optimization. Uncertainty aware optimization problems can be computationally complex due to the substantial number of model evaluations that are necessary to accurately quantify and propagate uncertainties. This computational complexity is greatly magnified if a high-fidelity, physics-based numerical model is used for the topology optimization calculations. Stochastic reduced order model (SROM) methods are applied here to effectively 1) alleviate the prohibitive computational cost associated with an uncertainty aware topology optimization problem; and 2) quantify and propagate the inherent uncertainties due to design imperfections.

A generic SROM framework that transforms the uncertainty aware, stochastic topology optimization problem into a deterministic optimization problem that relies only on independent calls to a deterministic numerical model is presented. This approach facilitates the use of existing optimization and modeling tools to accurately solve the uncertainty aware topology optimization problems in a fraction of the computational demand required by Monte Carlo methods. Finally, an example in structural topology optimization is presented to demonstrate the effectiveness of the proposed uncertainty aware structural topology optimization approach.

INTRODUCTION

The problem of interest in this study is a stochastic structural topology optimization problem in the case where the loading is considered to be random. The randomness in the loading will be introduced through uncertainty in the direction θ of an applied force. An optimal material distribution is sought by solving the following stochastic structural topology optimization problem

$$
\begin{aligned}
\min_{\boldsymbol{x}\in\mathbb{R}^{N_{\boldsymbol{x}}}} \; &: \; \mathcal{C}(\hat{\boldsymbol{x}}) = E\left[\boldsymbol{U}^T[\boldsymbol{K}(\hat{\boldsymbol{x}})]\boldsymbol{U}\right] = \sum_{e=1}^{N_e}(z_e(\hat{\boldsymbol{x}}_k))^\beta E\left[\bar{\boldsymbol{u}}_e^T[\boldsymbol{k}_e]\bar{\boldsymbol{u}}_e\right] \\
\text{subject to} \; &: \; \mathcal{R}(\boldsymbol{U},\hat{\boldsymbol{x}};\Theta) = \boldsymbol{0} \quad \text{in} \quad \Omega \quad \text{a.s.} \\
&: \; \sum_{e=1}^{N_e} z_e(\hat{\boldsymbol{x}}_k)V_e \leq V_{\max} \\
&: \; \boldsymbol{0} \leq \boldsymbol{x} \leq \boldsymbol{1},
\end{aligned}
\tag{1}
$$

where $\boldsymbol{x}$ denotes the density at the control points, $\hat{\boldsymbol{x}}$ is the filtered density at the control points, $\hat{\boldsymbol{x}}_k$ are the filtered densities associated with the k-th set of control points in finite element e, z_e is the filtered material density for element e, $\beta > 1$ is a penalty constant that aims to push the material density in element e to zero, N_e is the total number of finite elements, and $N_{\boldsymbol{x}}$ is the total number of control points. $\mathcal{C}$ is the expected value in the structural compliance, V_e is the volume of finite element e, and $V_{\max}$ is the material volume limit. $[\boldsymbol{K}]$ is the stiffness matrix assembled from element stiffness matrices $[\boldsymbol{k}_e]$ [1], $\boldsymbol{U}$ is the random global displacement vector and $\bar{\boldsymbol{u}}_e$ are the random displacements for element e, $\mathcal{R}$ is the residual equation, $\Omega \subseteq \mathbb{R}^d,\ d \in \{1,2,3\}$ is the computational domain, and Θ is the random direction of an applied force.

The volume constraint is defined using filtered material densities z_e but the filtered densities at the control points $\hat{\boldsymbol{x}}_e$ can be defined as nodal or element control points. Thus, given $\hat{\boldsymbol{x}}$, the filtered material density at each element is defined as:

$$
z_e(\boldsymbol{x}_k) = \frac{1}{\hat{n}_e}\sum_{k\in\mathcal{K}_e}\hat{\boldsymbol{x}}_k, \tag{2}
$$

where $\hat{n}_e$ is the number of control points in the set $\mathcal{K}_e$ of control points associated with element e. If nodal control points are used in (2), $\hat{n}_e$ is equal to the number of nodes on element e. Contrary, if element control points are used, $\hat{n}_e = 1$.

Notice that in (1) the stochastic structural topology optimization problem is now constrained by a system of stochastic algebraic equations

$$
\mathcal{R}(\boldsymbol{U},\hat{\boldsymbol{x}};\Theta) = [\boldsymbol{K}(\hat{\boldsymbol{x}})]\boldsymbol{U} - \boldsymbol{F}(\Theta), \tag{3}
$$

where $\boldsymbol{F}$ is the random global force vector. The global displacement and force vectors are now random in (3) through their dependence on the random direction of applied load Θ. The solution of (1) depends on a suitable parameterization of the random direction Θ so that the solution of the stochastic constraint equations and evaluation of the expected value in the structural compliance becomes tractable, discussed in Section 4.

The remainder of this article is organized as follows. In the next section, the motivation for this work is discussed. In the following section, the proposed method

is detailed, including the deterministic structural topology optimization formulation, a generic description of SROMs, and the presentation of the stochastic structural topology optimization formulation based on a SROM representation of the random direction Θ. The gradient derivation for the stochastic structural topology optimization problem using SROMs is also presented along with a summary of the core steps for computing the objective function and gradient. Finally, the paper is concluded with a summary of this work.

MOTIVATION

The intersection of additive processes and design optimization has introduced revolutionary capabilities for design, product development and manufacturing. "Complexity is free" has been a common mantra with additive manufacturing processes [2]. However, anyone involved in the qualification or certification of additive processes or materials will acknowledge that complexity is currently not free due to the prevailing lack of understanding of advanced manufacturing processes [2]. One approach to address the stochastic nature of additive processes is to improve process determinism. An alternate, complementary approach is to account for these inherent uncertainties early in the design process by providing designers with uncertainty aware computational design tools that generate solutions that insure performance requirements are met and margins are quantified.

Uncertainties are abound in any design scenario and include sources from requirements, boundary conditions and environments; not just process capabilities, feedstocks and final material properties. Advanced uncertainty quantification and propagation methodologies have been available for years [3, 4, 5], but even the most basic capabilities for design under uncertainty [6, 7, 8] remain unavailable to end users. Since existing tools do not account for uncertainties during analyses, there is no guarantee that their solutions are robust to these sources of uncertainty. While holding great potential and value for product performance and qualification, design under uncertainty is a significant challenge due to the computational resources necessary to create high-fidelity solutions. This computational toll limits the design iterations available to explore solutions robust to uncertainties. Thus, to make design under uncertainty an integral part of the design process, critical algorithmic issues must be solved. First, novel sampling algorithms are needed to reduce sample sizes required to accurately quantify and propagate sources of uncertainty. Second, algorithms must efficiently utilize all available computing resources to increase performance, speed, and accuracy. Third, these novel algorithms should be integrated into a reliable computational design tool accessible to end users.

This work aims to apply a stochastic reduced order model (SROM) to acount for uncertainty in applied loading during structural topology optimization. A SROM is a low-dimensional, discrete approximation to a continuous random element comprised of a finite and usually small number of samples with varying probability. This non-

intrusive approach enables efficient stochastic computations in terms of only a small set of samples and probabilities. The SROM concept was originally proposed in [9] and then further refined in [10]. The SROM approach has been demonstrated in multiple applications, including the determination of effective conductivities for random microstructures [11], the estimation of linear dynamic system states [12, 13], inverse problems under uncertainty [14], the quantification of uncertainty in intergranular corrosion rates [15], and the prediction of the structural reliability of components containing laser welds [16]. The primary strengths of SROMs are their ability to represent an underlying random quantity with low-dimensionality and to subsequently solve uncertainty propagation problems in a fraction of the computational time required by Monte Carlo methods.

This work, to the best of our knowledge, represents the first application of SROMs to structural topology optimization under uncertainty. Furthermore, by implementing this work in Sandia National Laboratories' Platform for Topology Optimization (PLATO) design tool [17], this represents the first implementation of SROMs in a production synthesis optimization tool. Today, PLATO users can apply this state-of-the-art SROM framework to solve structural topology optimization problems under uncertainty. The SROM framework represents a practical approach with the following strengths shown in this work: 1) it relies entirely on calls to existing deterministic solvers and optimization libraries, 2) it is easily parallelized and scalable, and 3) it is not specific to normally distributed random quantities. Additionally, in contrast with existing stochastic collocation-based methods that discretize the entire probability space equally, SROMs naturally give higher weight to important areas of the probability space [14]. This property yields low-dimensional approximations and thus relatively few calls to deterministic models.

FORMULATION

First, let $\mathbb{H} = L^2(\Omega; \mathbb{R}^d)$ denote the Hilbert space of measurable and square intregrable functions endowed with inner product $\langle \phi, \psi \rangle_{\mathbb{H}} = \int_\Omega \phi\, \psi$ for $\phi, \psi \in \mathbb{H}$ and norm $\|\phi\|_{\mathbb{H}} = \langle \phi, \phi \rangle_{\mathbb{H}}^{1/2}$ is defined. Now, define the finite dimensional spaces $\mathbb{U} := \text{span}\{\phi_\mathsf{i}\},\ \phi_\mathsf{i} \in \mathbb{H}$ for $\mathsf{i} = 1, \ldots \mathsf{I},\ \mathsf{I} \in \mathbb{N}$, $\mathbb{Y} := \text{span}\{\psi_\mathsf{j}\},\ \psi_\mathsf{j} \in \mathbb{H}$ for $\mathsf{j} = 1, \ldots \mathsf{J},\ \mathsf{J} \in \mathbb{N}$, and $\mathbb{V}_\mathsf{i} = \text{span}\{\varphi_\mathsf{k}\},\ \varphi_\mathsf{k} \in \mathbb{H}$ for $\mathsf{k} = 1, \ldots \mathsf{K},\ \mathsf{K} \in \mathbb{N}$. The following finite dimensional approximations for the displacements, control points, and Lagrange multipliers can then be defined as $\boldsymbol{u} = \sum_{\mathsf{i}=1}^{\mathsf{I}} a_\mathsf{i}\phi_\mathsf{i},\ a_\mathsf{i} \in \mathbb{R}\ \forall\ \mathsf{i} = 1, \ldots \mathsf{I}$, $\boldsymbol{x} = \sum_{\mathsf{j}=1}^{\mathsf{J}} b_\mathsf{j}\psi_\mathsf{j},\ b_\mathsf{j} \in \mathbb{R}\ \forall\ \mathsf{j} = 1, \ldots \mathsf{J}$, and $\boldsymbol{\lambda} = \sum_{\mathsf{k}=1}^{\mathsf{K}} c_\mathsf{k}\varphi_\mathsf{k},\ c_\mathsf{k} \in \mathbb{R}\ \forall\ \mathsf{k} = 1, \ldots \mathsf{K}$, respectively. This notation will be utilized in the formulation of the method throughout this section.

Deterministic Structural Topology Optimization

A typical deterministic structural topology optimization problem based on the Solid Isotropic Material with Penalization (SIMP) [18, 19] approach can be written as

$$\begin{aligned} \min_{\boldsymbol{x}\in\mathbb{R}^{N_{\boldsymbol{x}}}} \;&:\; \mathcal{C}(\hat{\boldsymbol{x}}) = \boldsymbol{u}^T[\boldsymbol{K}(\hat{\boldsymbol{x}})]\boldsymbol{u} = \sum_{e=1}^{N_e}(z_e(\hat{\boldsymbol{x}}_k))^\beta \boldsymbol{u}_e^T[\boldsymbol{k}_e]\boldsymbol{u}_e \\ \text{subject to} \;&:\; \mathcal{R}(\boldsymbol{u},\hat{\boldsymbol{x}};\theta) = \boldsymbol{0} \quad \text{in} \quad \Omega \\ &:\; \sum_{e=1}^{N_e} z_e(\hat{\boldsymbol{x}}_k)V_e \leq V_{\max} \\ &:\; \boldsymbol{0} \leq \boldsymbol{x} \leq \boldsymbol{1}, \end{aligned} \tag{4}$$

where

$$\mathcal{R}(\boldsymbol{u},\hat{\boldsymbol{x}};\theta) = [\boldsymbol{K}(\hat{\boldsymbol{x}})]\boldsymbol{u} - \boldsymbol{f}(\theta) \tag{5}$$

is the deterministic residual equation, $\boldsymbol{u}$ is the deterministic global displacement vector, and $\boldsymbol{f}$ is the global deterministic force vector resulting from a load in direction θ.

A parallel linear kernel was used to ensure existence of solutions and avoid numerical artifacts (e.g. checkerboard patterns) that may result from the discretization of the density field with possibly unstable finite elements. Specifically, a linear kernel filter

$$F_{ik} = \max\left(0, 1 - \frac{d(i,k)}{R}\right) \tag{6}$$

is applied to the control points [20, 21] to avoid the aforementioned numerical artifacts. Therefore, the filtered control point $\hat{\boldsymbol{x}}_k$ is given by

$$\hat{\boldsymbol{x}}_k = \sum_{i=1} = w^{ik}\boldsymbol{x}^i, \tag{7}$$

where the weights in (7) are defined as

$$w^{ik} = \frac{F_{ik}}{\sum_{l\in\mathcal{N}_k} F_{lk}}. \tag{8}$$

In equations (6)-(8), $d(i,k)$ is the distance between control points $\boldsymbol{x}^i$ and $\boldsymbol{x}^k$ and R is the radius of influence. $\mathcal{N}_k = \{\boldsymbol{x}^i \colon d(i,k) \leq R\}$ is the neighborhood of control points that are inside the radius R, including the control points on the boundary of the radius, with respect to control point $\boldsymbol{x}^k$.

Generic Description of SROM

A SROM is a discrete approximation of a random quantity (variable, vector, etc.) defined by a finite and generally small number of samples with varying probability. In this work, a SROM $\tilde{\Theta}$ defined by parameters $\{\tilde{\theta}^{(j)}, p^{(j)}\}_{j=1}^{m}$ is used as a low dimensional approximation of the random load direction Θ. Here, $\tilde{\Theta}$ has size m with samples $\{\tilde{\theta}^{(1)}, ..., \tilde{\theta}^{(m)}\}$ and probabilities $(p^{(1)}, ..., p^{(m)})$ associated with each sample, where $p^{(j)} \geq 0 \; \forall j$ and $\sum_{j=1}^{m} p^{(j)} = 1$. The cumulative distribution function (CDF), $\tilde{F}$, of the SROM is expressed as

$$\begin{aligned} \tilde{F}(\theta) &= P(\tilde{\Theta} \leq \theta) \\ &= \sum_{j=1}^{m} p^{(j)} \mathbf{1}\left(\tilde{\theta}^{(j)} \leq \theta\right), \end{aligned} \tag{9}$$

where $\mathbf{1}(\text{condition})$ is the indicator function ($= 1$ if the condition is true, $= 0$ otherwise), while q^{th} order moments are given by

$$\begin{aligned} \tilde{\mu}(q) &= E\left[\tilde{\Theta}^{q}\right] \\ &= \sum_{j=1}^{m} p^{(j)} (\tilde{\theta}^{(j)})^{q}. \end{aligned} \tag{10}$$

In practice, the SROM $\tilde{\Theta}$ must be formed such that it is close to Θ in a statistical sense. For a given random variable Θ with known CDF, $F(\theta)$, and moments, $\mu(q)$, this is done by selecting the defining SROM parameters through the following optimization problem

$$\begin{aligned} \tilde{\Theta} := \underset{\{\tilde{\theta}\}, \boldsymbol{p}}{\operatorname{argmin}} & \left(\alpha_1 \int_{I_\theta} \left(\tilde{F}(\theta) - F(\theta)\right)^2 d\theta + \alpha_2 \sum_{q=1}^{\bar{q}} \left(\frac{(\tilde{\mu}(q) - \mu(q))}{\mu(q)} \right)^2 \right) \\ \text{subject to}: \; & \sum_{j=1}^{m} p^{(j)} = 1 \text{ and } p^{(j)} \geq 0, \; j = 1, ..., m. \end{aligned} \tag{11}$$

Here, α_1 and α_2 are weighting factors controlling the relative importance of matching the target CDF and matching moments up to order $\bar{q}$, respectively, and $\int_{I_\theta}$ is the support of Θ. More details on the solution of the optimization problem in (11) can be found in [10].

After the SROM $\tilde{\Theta}$ has been determined through Equation (11), it can be used to efficiently and non-intrusively propagate uncertainty through a computational model such as Equation (3). In a manner analogous to Monte Carlo methods, this is done by first evaluating the deterministic model (Equation (5)) for values of Θ equal to each SROM sample, e.g.

$$\mathcal{R}(\boldsymbol{u}^{(j)}, \hat{\boldsymbol{x}}; \tilde{\theta}^{(j)}) = \mathbf{0}, \; j = 1, ..., m.$$

The resulting set of state samples, $\{\boldsymbol{u}^{(j)}\}_{j=1}^{m}$, and original probabilities, $\mathbf{p}$, define a SROM $\tilde{\boldsymbol{U}}$ for $\boldsymbol{U}$. The statistics of $\boldsymbol{U}$ can then be estimated using the analogous multidimensional versions of Equations (9) and (10). It has been shown in previous work [15, 10] that the number of model evaluations, m, required by SROMs can be substantially less than traditional Monte Carlo while retaining similar accuracy. In this way, SROMs can be viewed as a smart Monte Carlo method, where preprocessing is done through the optimization problem in Equation (11) to yield m samples of Θ with probabilities that are tuned to best reflect the original statistics.

Structural topology optimization using SROMs

A SROM $\tilde{\Theta}$ is first generated by solving (11) and optimizing for the defining parameters, $\{\tilde{\theta}^{(j)}, p^{(j)}\}_{j=1}^{m}$. The parameterization of the random direction, Θ, via SROM enables us to recast (1) as

$$\begin{aligned}
\min_{\boldsymbol{x}\in\mathbb{R}^N} \;:\; & \tilde{\mathcal{C}}(\hat{\boldsymbol{x}}) = E\left[\boldsymbol{U}^T[\boldsymbol{K}(\hat{\boldsymbol{x}})]\boldsymbol{U}\right] = \sum_{j=1}^{m} p^{(j)}(\tilde{\boldsymbol{u}}^{(j)})^T[\boldsymbol{K}(\hat{\boldsymbol{x}})]\tilde{\boldsymbol{u}}^{(j)} \\
& = \sum_{j=1}^{m} p^{(j)} \sum_{e=1}^{N} (z_e(\hat{\boldsymbol{x}}_k))^{\beta}(\tilde{\boldsymbol{u}}_e^{(j)})^T[\boldsymbol{k}_e]\tilde{\boldsymbol{u}}_e^{(j)} \\
\text{subject to} \;:\; & \mathcal{R}(\boldsymbol{u}^{(j)}, \hat{\boldsymbol{x}}; \tilde{\theta}^{(j)}) = \mathbf{0} \quad \text{in} \quad \Omega \quad \text{a.s., for } j = 1, ..., m \\
:\; & \sum_{e=1}^{N_e} z_e(\hat{\boldsymbol{x}}_k)V_e \leq V_{\max} \\
:\; & \mathbf{0} \leq \boldsymbol{x} \leq \mathbf{1},
\end{aligned} \tag{12}$$

where

$$\mathcal{R}(\boldsymbol{u}^{(j)}, \hat{\boldsymbol{x}}; \tilde{\theta}^{(j)}) = [\boldsymbol{K}(\hat{\boldsymbol{x}})]\tilde{\boldsymbol{u}}^{(j)} - \tilde{\boldsymbol{f}}^{(j)}. \tag{13}$$

In (13), $\tilde{\boldsymbol{f}}^{(j)} \equiv \boldsymbol{F}(\tilde{\theta}^{(j)})$ is the external force vector assembled using the jth sample of the SROM $\tilde{\Theta}$. Note that the stochastic algebraic constraint in Equation (1) has been transformed into a set of m independent deterministic constraint equations using the SROM. The decoupling of these equations allows them to be evaluated in parallel with simultaneous calls to the original deterministic model software.

Gradient Derivation

The adjoint approach based on a Lagrangian is used to derive the gradient of the objective function in (12) with respect to the control points $\boldsymbol{x}$. It is assumed that the objective function in (12) is differentiable with respect to $\boldsymbol{x}$ and that nodal values

of the control are used. First, the following Lagrangian function is defined

$$\mathcal{L}(\boldsymbol{x}, \tilde{\boldsymbol{\lambda}}^{(j)}) := \tilde{\mathcal{C}}(\hat{\boldsymbol{x}}) + (\tilde{\boldsymbol{\lambda}}^{(j)})^T([\boldsymbol{K}(\hat{\boldsymbol{x}})]\tilde{\boldsymbol{u}}^{(j)} - \tilde{\boldsymbol{f}}^{(j)}), \text{ for } j = 1, \ldots, m, \tag{14}$$

where $\tilde{\boldsymbol{\lambda}}^{(j)} \in \mathbb{R}^N$ denotes the j-th vector of Lagrange multipliers. Since $\mathcal{R}(\tilde{\boldsymbol{u}}^{(j)}, \hat{\boldsymbol{x}}; \tilde{\theta}^{(j)}) = 0$ is satisfied for all choices of $\tilde{\boldsymbol{\lambda}}^{(j)}$, the gradient of the objective function with respect to control points $\boldsymbol{x}$ is given by $\frac{d\mathcal{L}}{d\boldsymbol{x}}$. Therefore, using the fact that the displacement samples, $\{\tilde{\boldsymbol{u}}\}_{j=1}^m$, are viewed as implicit functions of $\boldsymbol{x}$, the derivative of (14) with respect to the design variables is given by

$$\begin{aligned}\frac{d\mathcal{L}(\boldsymbol{x}, \tilde{\boldsymbol{\lambda}}^{(j)})}{d\boldsymbol{x}_k} &= \frac{\partial \tilde{\mathcal{C}}(\hat{\boldsymbol{x}})}{\partial z_e}\frac{\partial z_e}{\partial \hat{\boldsymbol{x}}_k}\frac{\partial \hat{\boldsymbol{x}}_k}{\partial \boldsymbol{x}_k} + \frac{\partial \tilde{\mathcal{C}}(\hat{\boldsymbol{x}})}{\partial \tilde{\boldsymbol{u}}_e^{(j)}}\frac{\partial \tilde{\boldsymbol{u}}_e^{(j)}}{\partial \boldsymbol{x}_k} \\ &+ (\tilde{\boldsymbol{\lambda}}_e^{(j)})^T\left(\frac{\partial \mathcal{R}(\tilde{\boldsymbol{u}}^{(j)}, \hat{\boldsymbol{x}}; \tilde{\theta}^{(j)})}{\partial z_e}\frac{\partial z_e}{\partial \hat{\boldsymbol{x}}_k}\frac{\partial \hat{\boldsymbol{x}}_k}{\partial \boldsymbol{x}_k} + \frac{\partial \mathcal{R}(\tilde{\boldsymbol{u}}^{(j)}, \hat{\boldsymbol{x}}; \tilde{\theta}^{(j)})}{\partial \tilde{\boldsymbol{u}}_e^{(j)}}\frac{\partial \tilde{\boldsymbol{u}}_e^{(j)}}{\partial \boldsymbol{x}_k}\right),\end{aligned} \tag{15}$$

where (15) is explicitly expressed as

$$\begin{aligned}\sum_{j=1}^{m}\Bigg(&p^{(j)}\left(\beta(z_e(\hat{\boldsymbol{x}}_k))^{\beta-1}\frac{\partial z_e}{\partial \hat{\boldsymbol{x}}_k}\frac{\partial \hat{\boldsymbol{x}}_k}{\partial \boldsymbol{x}_k}(\tilde{\boldsymbol{u}}_e^{(j)})^T[\boldsymbol{k}_e]\tilde{\boldsymbol{u}}_e^{(j)}\right) \\ &+ (\tilde{\boldsymbol{\lambda}}_e^{(j)})^T\left(\beta(z_e(\hat{\boldsymbol{x}}_k))^{\beta-1}\frac{\partial z_e}{\partial \hat{\boldsymbol{x}}_k}\frac{\partial \hat{\boldsymbol{x}}_k}{\partial \boldsymbol{x}_k}[\boldsymbol{k}_e]\tilde{\boldsymbol{u}}_e^{(j)}\right) \\ &+ \left(p^{(j)}\left(2(z_e(\hat{\boldsymbol{x}}_k))^{\beta}[\boldsymbol{k}_e]\tilde{\boldsymbol{u}}_e^{(j)}\right) + (\tilde{\boldsymbol{\lambda}}_e^{(j)})^T(z_e(\hat{\boldsymbol{x}}_k))^{\beta}[\boldsymbol{k}_e]\right)\frac{\partial \tilde{\boldsymbol{u}}_e^{(j)}}{\partial \boldsymbol{x}_k}\Bigg).\end{aligned} \tag{16}$$

By using the adjoint approach, the third term in (16) can be eliminated by choosing the Lagrange multipliers such that they satisfy

$$(z_e(\hat{\boldsymbol{x}}_k))^{\beta}[\boldsymbol{k}_e]^T\tilde{\boldsymbol{\lambda}}_e^{(j)} = -p^{(j)}2(z_e(\hat{\boldsymbol{x}}_k))^{\beta}[\boldsymbol{k}_e]\tilde{\boldsymbol{u}}_e^{(j)}. \tag{17}$$

Therefore, the gradient of (14) is recast as

$$\begin{aligned}\sum_{j=1}^{m}\Bigg(&p^{(j)}\left(\beta(z_e(\hat{\boldsymbol{x}}_k))^{\beta-1}\frac{\partial z_e}{\partial \hat{\boldsymbol{x}}_k}\frac{\partial \hat{\boldsymbol{x}}_k}{\partial \boldsymbol{x}_k}(\tilde{\boldsymbol{u}}_e^{(j)})^T[\boldsymbol{k}_e]\tilde{\boldsymbol{u}}_e^{(j)}\right) \\ &+(\tilde{\boldsymbol{\lambda}}_e^{(j)})^T\left(\beta(z_e(\hat{\boldsymbol{x}}_k))^{\beta-1}\frac{\partial z_e}{\partial \hat{\boldsymbol{x}}_k}\frac{\partial \hat{\boldsymbol{x}}_k}{\partial \boldsymbol{x}_k}[\boldsymbol{k}_e]\tilde{\boldsymbol{u}}_e^{(j)}\right)\Bigg).\end{aligned} \tag{18}$$

Since $[\boldsymbol{k}_e]$ is self-adjoint and non-singular, the j-th Lagrange multipliers can be explicitly expressed as

$$\tilde{\boldsymbol{\lambda}}_e^{(j)} = -p^{(j)}2\tilde{\boldsymbol{u}}_e^{(j)}. \tag{19}$$

Thus, by substituting (19) into (18), the gradient of (14) can be expressed as

$$\sum_{j=1}^{m}\left(-p^{(j)}\left(\beta(z_e(\hat{\boldsymbol{x}}_k))^{\beta-1}\frac{\partial z_e}{\partial \hat{\boldsymbol{x}}_k}\frac{\partial \hat{\boldsymbol{x}}_k}{\partial \boldsymbol{x}_k}(\tilde{\boldsymbol{u}}_e^{(j)})^T[\boldsymbol{k}_e]\tilde{\boldsymbol{u}}_e^{(j)}\right)\right). \tag{20}$$

Finally, the derivative of the material volume constraint is given by

$$\frac{\partial z_e(\hat{\boldsymbol{x}}_k)}{\partial \hat{\boldsymbol{x}}_k}\frac{\partial \hat{\boldsymbol{x}}_k}{\partial \boldsymbol{x}_k}V_e. \tag{21}$$

Note that $\partial z_e(\hat{\boldsymbol{x}}_k)/\partial \hat{\boldsymbol{x}}_k = 1$ if element control points are used instead of nodal control points. Furthermore, $\partial \hat{\boldsymbol{x}}_k/\partial \boldsymbol{x}_k$ will depend on the type of kernel filter used to solve (12).

Implementation

In this section, the sequence of steps for computing the objective function and the gradient for the stochastic structural topology optimization problem defined in (12) is summarized. After solving the optimization problem in (11) for the SROM parameters, $\{\tilde{\theta}^{(j)}, m^{(j)}\}_{j=1}^m$, the following procedure is repeated to compute the objective function and gradient at each iteration:

1. Solve m decoupled, physics problems for the displacement samples, $\{\tilde{\boldsymbol{u}}^{(j)}\}_{j=1}^m$.
2. Evaluate the expected value in the structural compliance, $\tilde{\mathcal{C}}(\hat{\boldsymbol{x}})$.
3. Compute the gradient of the objective function using (20).

Notice that computing the objective function and its gradient at each iteration require m deterministic model evaluations. However, since the solves are decoupled and thus independent of each other, they can be easily parallelized to minimize computational cost. Furthermore, it is worth noting that the Hessian (or the application of the Hessian on a vector) can be easily derived along similar lines to the approach used for the deterministic case [22].

NUMERICAL EXAMPLE

In this section, the proposed SROM approach is used to solve a structural topology optimization problem where randomness is introduced through uncertainty in the direction of an applied external force. The SROM approach described in the previous section was implemented using the optimization toolbox in MATLAB [23]. The implementation is based on the fmincon function for constrained nonlinear optimization, which accepts the objective function (12) and gradient (20) to solve the stochastic structural topology optimization problem in (12). In all the examples presented herein, the interior-point algorithm was used along with a L-BFGS [24] Hessian approximation.

A sketch for the problem domain can be seen in Figure 1. The computational mesh with 150,126 eight-node hexahedron finite elements was created with Cubit [25]. The stochastic structural topology optimization problem was solved with PLATO [17]. Sierra Structural Dynamics [26] was used to solve the linear static problem in (13).

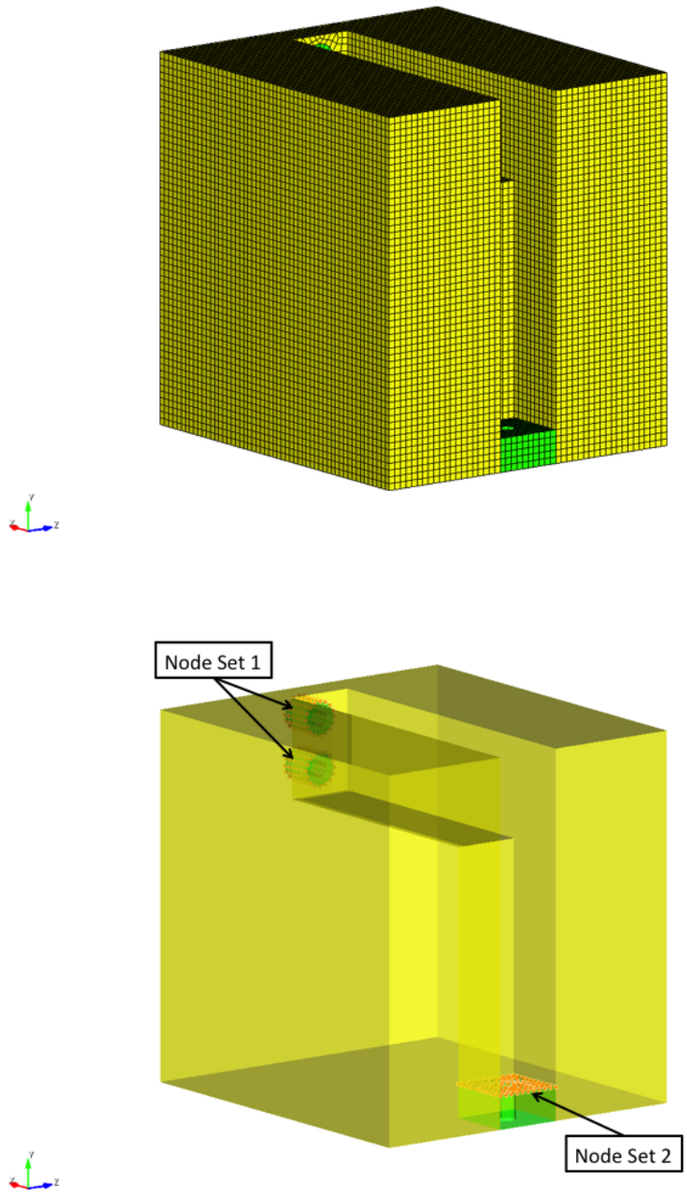

Figure 1: Problem domain used to solve the stochastic structural topology optimization problem. The top pane shows the computational mesh. The bottom pane shows the isosurface and the corresponding boundary conditions used to solve the stochastic structural topology optimization problem.

Fixed boundary conditions were applied on node set one, while a compressive force along the y-axis and with magnitude 10^5 was applied on node set two. The Young's modulus was set to 10^9 and the Poisson's ratio was set to 0.3.

The SROM approach was used to solve (12) when considering randomness in the direction of the applied load for the optimal samples and probabilities, $\{\tilde{\theta}^{(j)}, p^{(j)}\}_{j=1}^{m}$. The target probability distribution for the random direction was a standard beta distribution, beta(3.6825,9.2063), on the interval $[60^\circ\ 100^\circ]$. The volume fraction was set to seven percent of the original volume ($\gamma = 0.07$). The optimality criteria algorithm [27] in PLATO was used to solve (12). The algorithm was terminated based on a tolerance on the relative change in the solution between iterations or the maximum number of iterations, specified as $\epsilon \leq 10^{-2}$ or 100, respectively. The initial guess for each design variable, i.e. $\boldsymbol{x}_e$, was set to the target volume fraction. The filter's radius of influence was set to two times the smallest element length, i.e. $R = 2\ell_e$.

The first step was to generate the SROM $\tilde{\Theta}$ for the random direction of the applied load, which was done offline as a preprocessing step before the stochastic structural topology optimization problem is solved. With the known expressions for the beta random variable statistics, the SROM optimization problem in (11) for uncertainty propagation in forward models is solved to generate $\tilde{\Theta}$ for a range of model sizes $m = \{5, 10, 15, 20\}$. The CDF and moment error terms, (9) and (10) respectively, are given equal weight in the objective function in (11), i.e. $\alpha_1 = \alpha_2 = 1.0$. The convergence of the load SROM construction problem with increasing SROM size, m, is shown in Figure 2. It is clearly seen that with further refinement of the $\tilde{\Theta}$ SROM, the

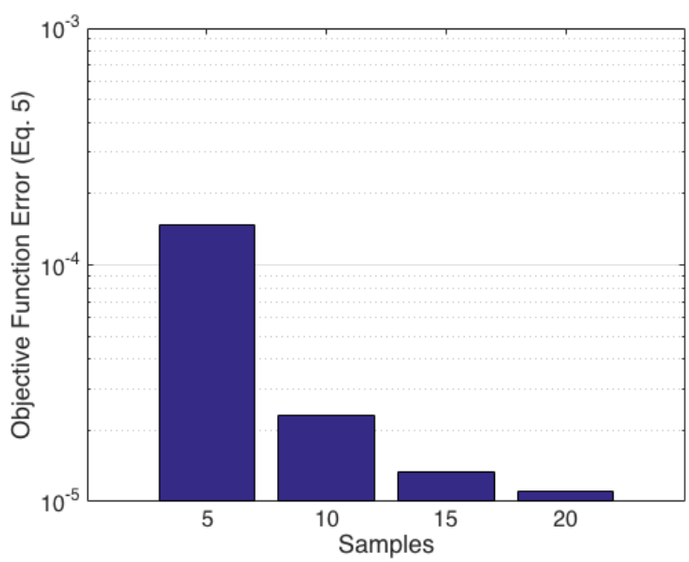

Figure 2: Convergence of the SROM construction problem (11) with increasing SROM size when generating the SROM for the random direction of the applied load.

statistics of the underlying random loading direction is better approximated. Note that the computational cost of the stochastic structural topology optimization problem increases proportionally to the size of the SROM used. Therefore, the smallest SROM representation yielding an acceptable error should be used in practice to minimize the computational cost associated with (12). In Figure 3, the SROM CDF approximation for different sizes is compared to the true distribution for the direction of the applied load. It is clear that the discrete nature of the SROM approximation improves with increased SROM size.

Next, lets study the behavior of the objective function (11) for increasing SROM size as shown in Figure 2. As expected, the objective function value decreases with increasing SROM size. A SROM $\tilde{\Theta}$ with more parameters should be capable of better approximating the statistics in Θ. From Figure 2, it is seen that a relatively small number of samples and probabilities defining $\tilde{\Theta}$ were able to produce a small discrepancy

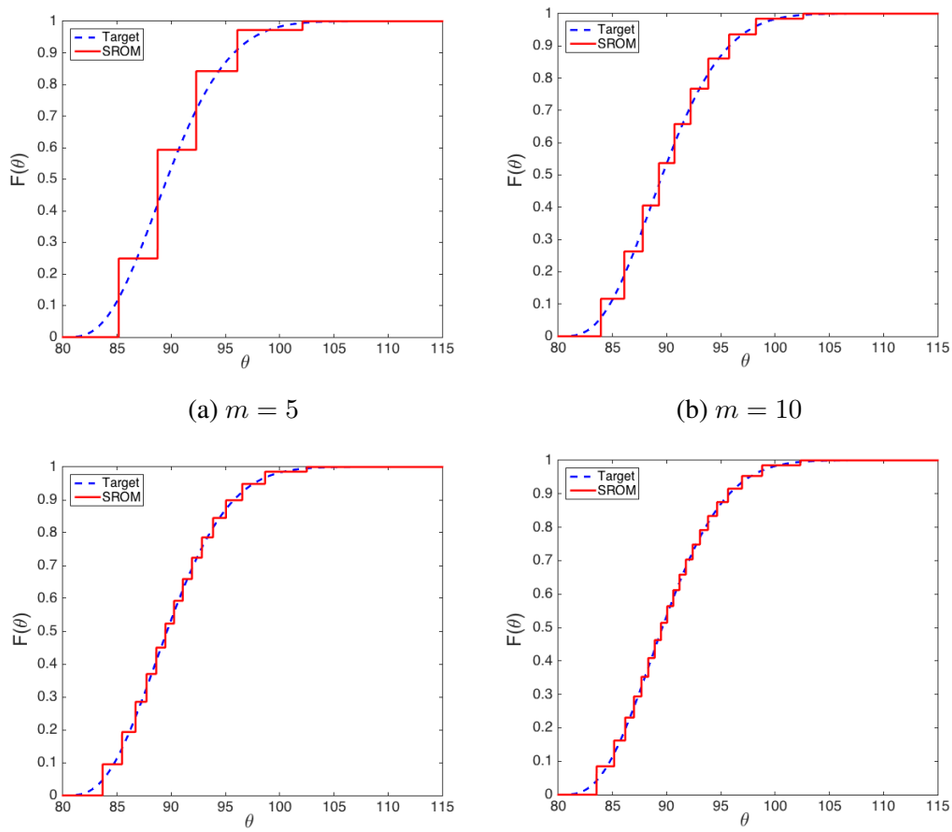

(a) $m = 5$ (b) $m = 10$

(c) $m = 15$ (d) $m = 20$

Figure 3: Comparison of the SROM CDFs with the true distribution of the direction of the applied load (Θ) for different SROM sizes.

between computed and observed moments. Indeed, very little improvement in the final objective function value is observed as the SROM size is increased from 15 to 20.

Finally, in Figure 4[1], the optimal topology obtained by solving (12) with different SROM sizes is compared to the optimal topology obtained by solving (4). These components represent those that are expected to be the least compliant (stiffest) under the prescribed volume constraints when node set 1 in Figure 1 is constrained and node set 2 is subject to a loading with random orientation. In Figure 4 it can be seen that the deterministic and the uncertainty aware structural topology optimization problems yield different solutions. The deterministic solution is symmetric about the y-axis; however, the uncertainty aware solution looses its symmetry about the y-axis due to the randomness in the direction of the applied load. Indeed, more material is placed on the right side of the structure to counter the fact that the distribution on the direction of the applied load favors samples above $90°$. Therefore, the right side of the structure is more likely to carry a greater share of the load than the left side of the structure. Furthermore, unlike the deterministic problem in which the load is perfectly applied along the y-axis, the stochastic solutions have additional support material between the two main structural members. This support material was likely placed to counter the possibility of these members buckling due to an asymmetric load. Therefore, the rigidity (i.e. stiffness) of the structure is increased by placing additional support material between the two main structural members. This highlights the importance of taking into account inherent design uncertainties when designing a structure since a small misalignment in the orientation of the applied load could prompt failure due to buckling.

CONCLUSION

In this study, a novel framework for structural topology optimization under uncertainty using stochastic reduced order models (SROMs) was proposed. By considering the structural topology optimization problem as a constrained stochastic optimization problem, the approach was formulated in terms of minimizing an abstract objective function with a stochastic model constraint. The non-intrusive nature of the SROM approximation transforms the constrained stochastic optimization problem into a deterministic one with decoupled, deterministic physics model constraints. Therefore, the use of SROMs allows for a widely applicable method that relies solely on calls to existing deterministic analysis solvers and optimization libraries. Furthermore, since the model evaluations are completely independent from one another, the approach is embarrassingly parallel and hence scalable to large design problems.

The effectiveness of the proposed SROM framework on a structural topology optimization problem with random loading was demonstrated. Through a numerical example, the importance of taking into account inherent uncertainties due to design imperfections when designing a structure was shown. Furthermore, the approach can

[1]PLATO normalizes the objective function values with respect to the objective function value of the first optimization iteration.

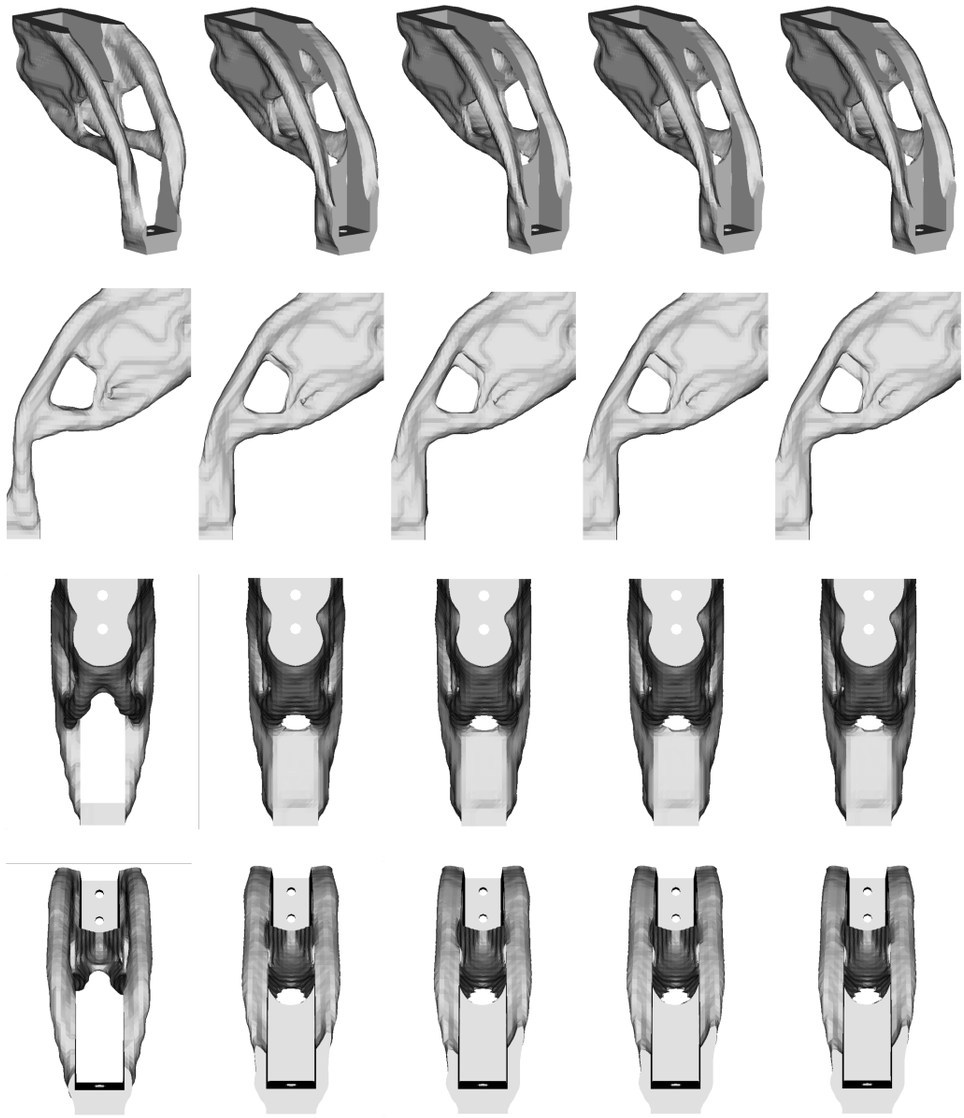

(a) Deterministic (b) $\tilde{\Theta} = 5$ (c) $\tilde{\Theta} = 10$ (d) $\tilde{\Theta} = 15$ (e) $\tilde{\Theta} = 20$

Figure 4: The optimized topology for increasing SROM sizes. (a) First column is the deterministic solution ($\tilde{\mathcal{C}} = 7.05e^{-4}$); (b) second column is the optimized topology for a SROM of size five ($\tilde{\mathcal{C}} = 7.23e^{-4}$); (c) third column is the optimized topology for a SROM of size ten ($\tilde{\mathcal{C}} = 7.21e^{-4}$); (d) fourth column is the optimized topology for a SROM of size fifteen ($\tilde{\mathcal{C}} = 7.23e^{-4}$); and (e) fifth column is the optimized topology for a SROM of size twenty ($\tilde{\mathcal{C}} = 7.23e^{-4}$).

accurately and efficiently quantify and propagate the statistics of a random load during optimization. The method requires a small number of samples to characterize the statistics of a random input, drastically reducing the computational cost associated with the stochastic structural topology optimization problem.

ACKNOWLEDGMENT

Sandia National Laboratories is a multi-program laboratory managed and operated by Sandia Corporation, a wholly owned subsidiary of Lockheed Martin Corporation, for the US Department of Energy's National Nuclear Security Administration under contract DEAC04-94AL85000. The information provided in this paper is the sole opinion of the authors and does not necessarily reflect the views of the sponsoring agencies. This document has been reviewed and approved for unclassified, unlimited release under SAND2017-xxxxA.

REFERENCES

Hughes, T. J., 2012. *The finite element method: linear static and dynamic finite element analysis*. Courier Corporation.

Jared, B. H., Aguilo, M. A., Beghini, L. L., Boyce, B. L., Clark, B. W., Cook, A., Kaehr, B. J., and Robbins, J., 2017. "Additive manufacturing: Toward holistic design". *Scripta Materialia*.

Ghanem, R. G., and Spanos, P. D., 2003. *Stochastic finite elements: a spectral approach*. Courier Corporation.

Babuška, I., Tempone, R., and Zouraris, G. E., 2004. "Galerkin finite element approximations of stochastic elliptic partial differential equations". *SIAM Journal on Numerical Analysis,* ***42***(2), pp. 800–825.

Babuška, I., Nobile, F., and Tempone, R., 2007. "A stochastic collocation method for elliptic partial differential equations with random input data". *SIAM Journal on Numerical Analysis,* ***45***(3), pp. 1005–1034.

Frangopol, D. M., 1995. "Reliability-based optimum structural design". In *Probabilistic structural mechanics handbook*. Springer, pp. 352–387.

Maute, K., and Frangopol, D. M., 2003. "Reliability-based design of mems mechanisms by topology optimization". *Computers & Structures,* ***81***(8), pp. 813–824.

Kharmanda, G., Olhoff, N., Mohamed, A., and Lemaire, M., 2004. "Reliability-based topology optimization". *Structural and Multidisciplinary Optimization,* ***26***(5), pp. 295–307.

Grigoriu, M., 2009. "Reduced order models for random functions. application to stochastic problems". *Applied Mathematical Modelling,* ***33***(1), pp. 161–175.

Warner, J. E., Grigoriu, M., and Aquino, W., 2013. "Stochastic reduced order models for random vectors: application to random eigenvalue problems". *Probabilistic Engineering Mechanics,* ***31***, pp. 1–11.

Grigoriu, M., 2010. "Effective conductivity by stochastic reduced order models (sroms)". *Computational Materials Science,* ***50***(1), pp. 138–146.

Grigoriu, M., 2010. "Linear random vibration by stochastic reduced-order models". *International journal for numerical methods in engineering,* ***82***(12), pp. 1537–1559.

Grigoriu, M., 2013. "Solution of linear dynamic systems with uncertain properties by stochastic reduced order models". *Probabilistic Engineering Mechanics,* ***34***, pp. 168–176.

Warner, J. E., Aquino, W., and Grigoriu, M., 2015. "Stochastic reduced order models for inverse problems under uncertainty". *Computer Methods in Applied Mechanics and Engineering,* ***285***, pp. 488–514.

Sarkar, S., Warner, J. E., Aquino, W., and Grigoriu, M. D., 2014. "Stochastic reduced order models for uncertainty quantification of intergranular corrosion rates". *Corrosion Science,* ***80***, pp. 257–268.

Emery, J. M., Field, R. V., Foulk, J. W., Karlson, K. N., and Grigoriu, M. D., 2015. "Predicting laser weld reliability with stochastic reduced-order models". *International Journal for Numerical Methods in Engineering,* ***103***(12), pp. 914–936.

Plato, 2017. Sandia National Laboratories, Plato. `http://www.sandia.gov/plato3d/index.html`. Accessed: 2016-12-06.

Bendsoe, M. P., and Sigmund, O., 2013. *Topology optimization: theory, methods, and applications*. Springer Science & Business Media.

Bendsoe, M. P., 1995. *Optimization of structural topology, shape, and material*, Vol. 414. Springer.

Bourdin, B., 2001. "Filters in topology optimization". *International Journal for Numerical Methods in Engineering,* ***50***(9), pp. 2143–2158.

Bruns, T. E., and Tortorelli, D. A., 2001. "Topology optimization of non-linear elastic structures and compliant mechanisms". *Computer Methods in Applied Mechanics and Engineering,* ***190***(26), pp. 3443–3459.

Heinkenschloss, M., 2008. Numerical solution of implicitly constrained optimization problems. TR08-05, Rice University, 6100 Main Street, Houston, TX 77005-1892.

MATLAB, 2015. The MathWorks Inc. Natick, Massachusetts. MATLAB Version 8.5.0 (R2015a).

Liu, D. C., and Nocedal, J., 1989. "On the limited memory BFGS method for large scale optimization". *Mathematical programming,* ***45***(1), pp. 503–528.

Cubit Team, 2016. "Cubit, geometry and mesh generation toolkit: version 15.2 user's manual". *Sandia National Laboratories, Tech. Rep. SAND2016-1649 R*.

Sierra Structural Dynamics Development Team, 2015. "Sierra structural dynamics - user's notes". *Sandia National Laboratories, Tech. Rep. SAND2015-9132*.

Sigmund, O., 2001. "A 99 line topology optimization code written in Matlab". *Structural and Multidisciplinary Optimization,* ***21***(2), pp. 120–127.